Triton X-100 concentration effects on membrane permeability of a single HeLa cell by scanning electrochemical microscopy (SECM)

Dipankar Koley and Allen J. Bard[1]

Center for Electrochemistry, Department of Chemistry and Biochemistry, University of Texas at Austin, 1 University Station, A5300, Austin, TX 78712-0165

Contributed by Allen J. Bard, August 6, 2010 (sent for review April 7, 2010)

Changes in HeLa cell morphology, membrane permeability, and viability caused by the presence of Triton X-100 (TX100), a nonionic surfactant, were studied by scanning electrochemical microscopy (SECM). No change in membrane permeability was found at concentrations of 0.15 mM or lower during an experimental period of 30 to 60 min. Permeability of the cell membrane to the otherwise impermeable, highly charged hydrophilic molecule ferrocyanide was seen starting at concentrations of TX100 of about 0.17 mM. This concentration level of TX100 did not affect cell viability. Based on a simulation model, the membrane permeability for ferrocyanide molecules passing though the live cell membrane was 6.5± 2.0×10^{-6} m/s. Cells underwent irreversible permeabilization of the membrane and structural collapse when the TX100 concentration reached the critical micelle concentration (CMC), in the range of 0.19 to 0.20 mM. The impermeability of ferrocyanide molecules in the absence of surfactant was also used to determine the height and diameter of a single living cell with the aid of the approach curve and probe scan methods in SECM.

live and intact cells | hydrophilic molecules | Comsol Multiphysics Simulation

Detergents are widely used in biology for protein extraction from cell membranes, in the crystallization of proteins, as stabilizing and denaturing agents, and as membrane permeabilizing agents. Triton X-100 (TX100) is one of the most widely used nonionic surfactants for lysing cells to extract protein and other cellular organelles or to permeabilize the living cell membrane for transfection (1–3). However, if large amounts are added or the cells are subject to prolonged exposure to TX100, the cells die (4–7). This toxicity of TX100 molecules arises because of the disrupting action of its polar head group on the hydrogen bonding present within the cell's lipid bilayer, leading to the destruction of the compactness and integrity of the lipid membrane. The insertion of detergent monomer into the lipid membrane begins at low concentrations. This leads to a disruption of cellular structure and eventual overpermeabilization of the cell membrane at concentrations above the critical micelle concentration (CMC) from the bilayer–micelle transition. Because cell viability is extremely sensitive within a narrow range of surfactant concentrations, especially near LD_{50}, controlling the TX100 concentration for transfection, e.g., the introduction of hydrophilic species without damaging cells, is difficult. Moreover, cholesterol or similar molecule-rich membrane domains are reported to be more tolerant toward detergents such as TX100 molecules in comparison to other parts of the lipid bilayer. (8–14).

Scanning electrochemical microscopy (SECM) has found increasing application in recent years to the study of living cells as well as biological systems in general (15). A number of studies have dealt with the permeability of redox species into the live cell. These have shown that highly charged hydrophilic molecules such as $Ru(NH_3)_6^{3+}$, $Ru(CN)_6^{4-}$, $Fe(CN)_6^{4-}$, and $Fe(CN)_6^{3-}$, as well as ferrocene carboxylate, cannot penetrate the intact cell membrane while hydrophobic molecules such as menadione, 1,2-napthaquinone, and MV^{2+} can. Thus while the molecules ferrocene methanol and tetramethyl-*p*-phenylenediamine (TMPD) show positive feedback behavior in SECM, signaling reduction of the oxidized form from interacting with the cell, molecules such as $Co(bpy)_3^{2+}$ and $Co(phen)_3^{2+}$, show negative feedback over live HeLa cells. Redox molecules inside the cell have also been shown to exchange electrons with redox molecules outside the membrane in the solution (16). SECM has also been used to find the local permeability of an isolated Xenopus oocyte nucleus for redox molecules as $>9.8 \times 10^6$ molecules/Nuclear. Pore Complex (NPC)/s (17). Fully automated time lapse SECM monitored single Hep G2 cell topography in the presence of antifreeze proteins over a period of 8 h at 4 °C (18). SECM has also been used in the induced transfer mode to measure the permeability of MV^{2+} through bovine articular cartilage, while topographic information was obtained with the membrane impermeable to $Ru(CN)_6^{4-}$ as a redox mediator (19). Heterogeneity in the permeability of oxygen across cartilage has also been observed by SECM imaging especially near the μm-size cellular and pericullar domain (20).

Although there have been many quantitative studies of the TX100 molecule and its interaction with artificial lipid bilayers (21–25), there have been none with a living cell membrane and its behavior in terms of its permeability, morphology, and metabolic behavior in real time. We report here how the single live cell permeability and morphology are affected by TX100, the most commonly used surfactant for permeabilization in many fluorescent and toxicological studies. Most modern studies are based on fluorescent tagging of antibodies in which one of the essential steps involved is to permeabilize the cell membrane by a surfactant to access the cellular interior targeted by the antibody fluorescent tag. Yet little is known about what happens to the cell when its membrane is permeabilized. Moreover, almost all the studies have been designed to show the permeability of redox species, but there are no reports on the effect of nonelectroactive species on cellular permeability. In this work we provide quantitative data on the permeability of the cell membrane in the presence of nonelectroactive molecules like TX100 as well as how this permeability actually affects the hydrophobicity of the cellular membrane.

Results

Fluorescence-Based Cell Viability. The cytotoxicity of TX100 on HeLa cells were recorded at different concentrations for 5, 10 and 15 min (Fig. S1*A*). The TX100 molecules were known to form micelles in the 0.22 to 0.24 mM range (26). In our cytotoxic test the cell viability dropped sharply when the TX100 concentration

Author contributions: D.K. and A.J.B. designed research; D.K. performed research; D.K. and A.J.B. analyzed data; and D.K. and A.J.B. wrote the paper.

The authors declare no conflict of interest.

[1]To whom correspondence should be addressed. E-mail: ajbard@mail.utexas.edu.

This article contains supporting information online at www.pnas.org/lookup/suppl/doi:10.1073/pnas.1011614107/-/DCSupplemental.

reached close to the CMC. Because the viability test was based on the integrity of the cell membrane, the micelle clearly showed a greater detergent action on the lipid bilayer than the individual surfactant molecule and hence was more toxic (27). Thus most of the studies by SECM were performed in the concentration range below the CMC to have enough time to observe the permeabilizing action on the cellular membrane by TX100 molecules.

Cellular Topography Without Surfactant. HeLa cells, when alive, are anchored to the surface of the Petri dish and tend to be stretched out to maintain their normal cellular functions. Hence with the aid of SECM, the height and diameter of the cells on the dish surface could be measured. Fig. 3 shows the cellular topography obtained from an x-scan SECM experiment. Here, a highly hydrophilic charged ion like ferrocyanide, and hence impermeable, was used as redox mediator. When the tip was scanned over the cell (Fig. 3*A*), the diffusion of ferrocyanide molecules to the tip was blocked (so-called negative feedback) (15) depending on the topographical variation of the living cell, so the diameter, shape, and size of the cell could easily be determined. X-scan data, i.e., current vs. absolute distance in the x-direction scan (Fig. 3*B*), can be converted to cellular height vs. absolute x-direction distance with the aid of a simulated negative feedback approach curve on the dish. By using experimental data, cell height was determined to be 9 to 12 μm and the diameter was in the range of 50 to 60 μm. Simulated x-scan data was fitted with the experimental data with a precision range of ±1 μm (Fig. 3*B*).

Because SECM gives z-direction topographic feature information very accurately, approach curves on a single cell were carried out to obtain additional cell heights. Fig. 3*D* shows the comparative approach curve on the dish and single cells. To confirm the cell height the simulated approach curve had been fitted with both experimental approach curves. From the fitting in Fig. 3*D* the cell height was 14 ± 1 μm. Details about the Comsol Multiphysics Simulation model and parameters (Fig. S4) can be found in *SI Text*.

Cell Membrane Permeability. SECM scans as above were carried out in the presence of TX100. Here, the 10 μm Pt tip was scanned in the x-direction over a single cell at a fixed height of approximately 16 μm and at a potential of 0.35 V. The current-distance profile with respect to time in the presence of 0.17 mM and 0.19 mM TX100 and 4 mM ferrocyanide was obtained as shown in Fig. 4 *A* and *B*. The normalized minimum current or the peak current against the background current from the x-scan was plotted against time, including results with 1.9 mM TX100, is shown in Fig. 4*C*. In the presence of 0.19 mM of TX100 (Fig. 4*C*) the normalized peak current went to the background current ($i_{T,\infty}$) within 2 min. This result clearly indicates that TX100 at these concentrations was lethal to cells causing the cell membrane to break apart and detach completely from the surface of the Petri dish. When 0.17 mM TX100 was added, however, the normalized minimum current decreased about 20% from the pre-TX100 treatment before essentially recovering after about 20 min in some cases. The recovery period and state of recovery varied from cell to cell as shown in Fig. 4*C*. The observed current decrease could be attributed to either an increase in permeability of the cell membrane or to an increase in topographical height. If the permeability increase model was correct, then the decrease was due to competitive consumption of ferrocyanide molecules both by SECM tip and by the cell. The rise of minimum current or the peak current to the pre-TX100 current level after 20–30 min may signal the cessation of competitive consumption of ferrocyanide molecules. This would indicate recovery of the cell membrane from the permeabilization action of 0.17 mM TX100 without the cell dying.

The cell height and topographic features from the x-scan in the absence of surfactant yielded a cell diameter and height of 50 μm and 10 μm, respectively. Permeability parameters for the cell membranes or boundaries were then introduced into the simulation model. The simulated x-scan data was then fitted with the experimental data at the same fixed height. Because the permeability changed with the exposure time of cells to 0.17 mM TX100, simulations were done to fit each curve to determine the permeability of the membrane at that particular time. This gave a range of permeability values from 4.0 to 8.7×10^{-6} m/s for the ferrocyanide molecules permeating through a live cell membrane. Hence, with the average permeability value of $6.5 \pm 2.0 \times 10^{-6}$ m^2/s, number of ferrocyanide molecules inside a single

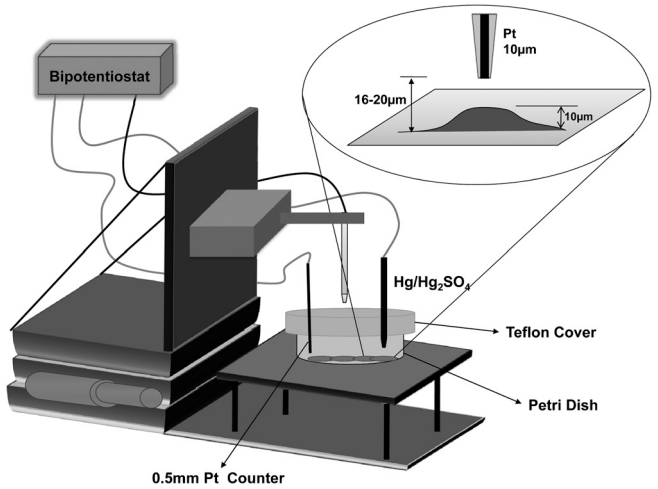

Fig. 1. Experimental setup for SECM experiment. The tip used was 10 μm Pt (RG ~ 5). Counter and reference electrode was 0.5 mm Pt wire and Hg/Hg_2SO_4 respectively.

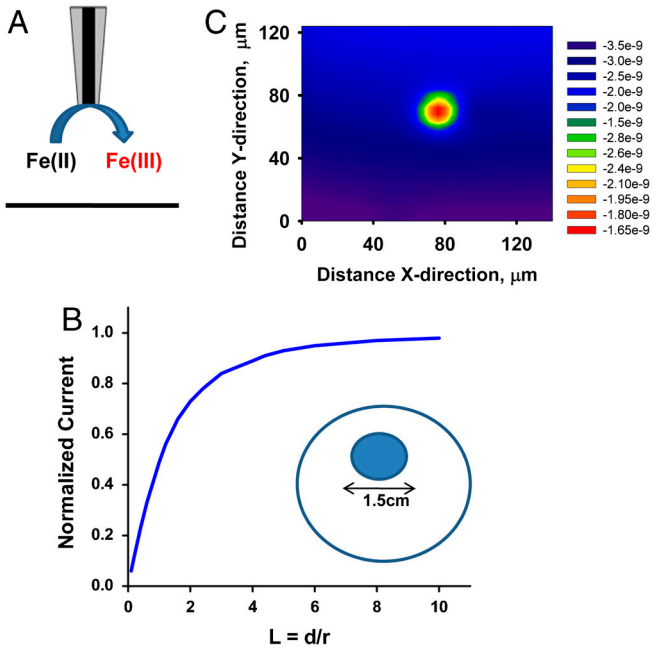

Fig. 2. (*A* and *B*) 4 mM ferrocyanide was used as redox couple to perform the negative feedback approach curve on the petri dish. (*Inset*) HeLa cells were cultured in a 1.5 cm spot on a Petri dish. (*C*) SECM image of a single living HeLa cell (red circle). Lower current (red color) over the cell signifies the cell was sticking out of the dish. Cells were found and identified by SECM image at a constant height of 16 μm away from dish and at +0.5 V potential vs. Hg/Hg_2SO_4 in presence of 4 mM of ferrocyanide in HEPES buffer (as described in cell culture subsection).

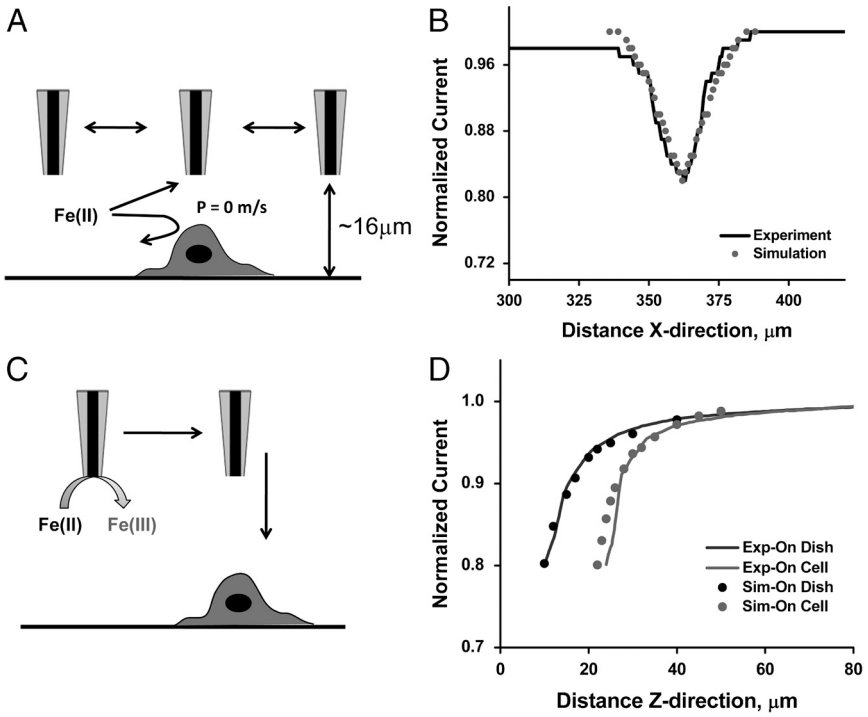

Fig. 3. (*A*) Tip-dish distance was adjusted to approximately 16 μm and then scanned over a single cell in x-direction at $E_T = 0.5$ V with 4 mM of ferrocyanide in solution. (*B*) Cellular topography observed by x-scan experiment (solid line) on single cell at $E_T = 0.5$ V with 4 mM ferrocyanide in buffer. The x-axis distance was an arbitrary unit. Y-axis current was normalized against background current over dish. The simulated x-scan data fit with experiment data for the following simulation parameters: tip: 10 μm (RG = 10); bulk concentration: 4 mM; tip-dish distance: 16 μm; cell diameter: 60 μm; cell height: 9.8 μm. The simulation was performed in 2D-axial symmetry using Fick's second law of diffusion. The cell height was determined by simulated data fitting with experimental ones. (*C*) Approach curves over dish and over single cell at $E_T = 0.5$ V with 4 mM ferrocyanide in buffer. (*D*) Experimental approach curves on dish and HeLa cell compared to simulated approach curves for total negative feedback.

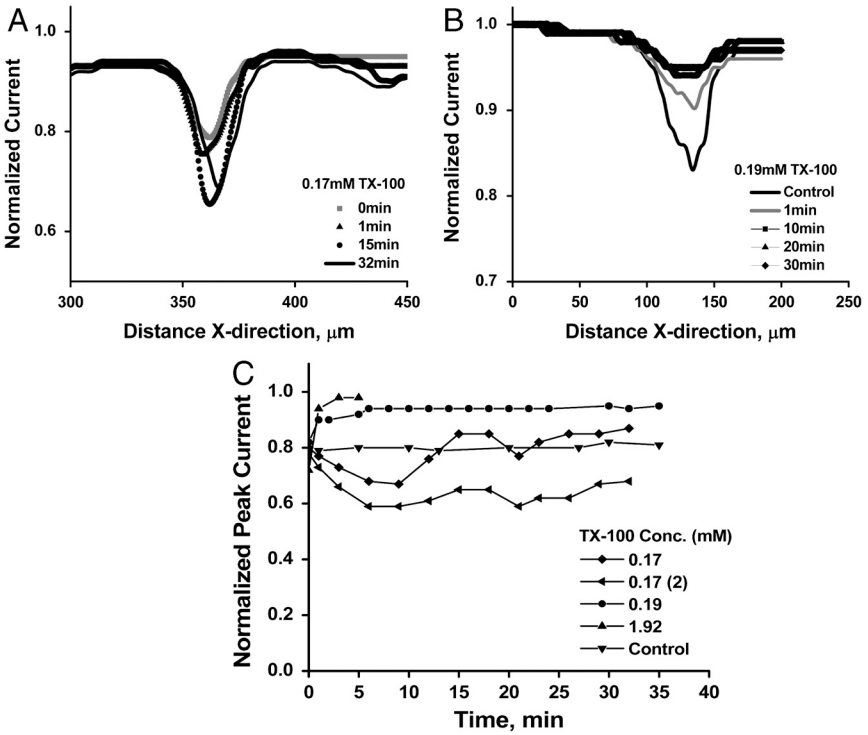

Fig. 4. X-scan experiments with (*A*) 0.17 mM or (*B*) 0.19 mM TX100 and 4 mM ferrocyanide in solution. (*C*) Normalized peak current was plotted against time for different concentrations of TX100 exposed to HeLa cell. Permeability of a single cell in presence of 0.17 mM TX100 was fitted to be $6.5 \pm 2.0 \times 10^{-6}$ m/s.

cell after 32 min was determined to be $1.06 \pm 0.54 \times 10^6$ in presence of 0.17 mM TX100. This model assumed that the cells maintained their integrity, i.e., the cell height and diameter were constant throughout the experiment. The permeability, P, is defined here as the velocity of a molecule of interest through a membrane; where $P = KD/L$, K is the partition constant between the molecule and the membrane, D is the diffusion coefficient of the molecule, and L is the length through which the molecule travels, i.e., the thickness of the membrane. Because the SECM tip was always held at the potential for ferrocyanide oxidation, the tip was not sensitive to ferricyanide, so only the ferrocyanide molecules permeating through the cell membrane effect the SECM tip current. Details of the simulation model (Fig. S4) are given in *SI Text*.

Cellular Topography in Presence of TX100. SECM approach curves have been used in many previous studies to estimate surface topography. During the probe scan experiment the tip was moved over the cell at a very slow scan rate (~5 μm/s). The decrease of current that was observed might have occurred due to an increase in cell height, e.g., by swelling of the cell volume, but may also have been caused by changes in permeability of the membrane. To distinguish between these effects, time dependent approach curves on a single cell were performed in the presence of different concentrations of TX100 as shown in Fig. S2*A*. For a z-scan rate of approximately 5 μm/s, the time to record a single approach curve takes about 20 sec. Fig. S2*B* represents the actual cell height variation with time. The cell height was taken as the difference between the approach curve to the Petri dish and to single cell. The average cell height was 10 ± 2 μm. Cells exposed to 0.17 mM or less of TX100 solution, the z-direction topography, and the cellular height did not change significantly from that in its absence. When 0.19 mM of TX100 was added, the cells started losing their topographical features as seen in Fig. S2*B*, where the cell height approached zero after 30 min of exposure to 0.19 mM of TX100. This shows a loss of viability at this concentration, as also observed in the fluorescence-based viability tests (Fig. S1). This demonstrates that obtaining SECM approach curves on a single cell is a good technique to monitor the cell height.

Current-time (i_T vs. t) Response Over a Single Cell. These curves were taken to study effects at longer times. Fig. S3*B* shows a i_T vs. t response curve when the 10 μm tip was held approximately 5 μm away from the surface of the cell in presence of 4 mM ferrocyanide and 0.17 mM TX100. The current recorded was plotted against time with the tip both above the cell and at approximately 500 μm away from the dish (Fig. S3*C*). The current above the cell decreases with time while the bulk current remains constant throughout the experimental time period. This indicates that the cells consume ferrocyanide molecules competitively with the tip held at the diffusion-controlled potential. No change in the cell height was also confirmed from the approach curve before and after 40 min of exposure of 0.17 mM TX100 (Fig. S3*D*).

Discussion

When the concentration of TX100 is below the CMC range (i.e. 0.17 mM and less) the surfactant may act as a permeabilizing agent depending on the dose and duration of exposure to cells. This is a good range for transfection of the cell with an added agent, but prolonged exposure to cells even at these low concentrations can lead to some cell death. When concentrations of TX100 in the CMC range, >0.18 mM, are used, the cell membrane disintegrated causing a collapse of the entire cell structure and cell death within a few minutes.

SECM allows one to follow a series of changes a cell undergoes in terms of its size, shape, and membrane permeability. At 0.17 mM or lower TX100 concentration provides enough time to study the cell behavior and allows interpretation of the data. When 0.17 mM TX100 solution is added to the cell, the membrane first becomes permeabilized sufficiently to allow hydrophilic molecules, like ferrocyanide, to permeate the cell membrane, while the cell height remains unaffected. Even when exposed for a long time (≥20 min) cells recover from membrane damage after the surfactant is removed. Occasionally the cell undergoes a reduction in height during its recovery from periods of increased permeability. When 0.20 mM TX100 is added, the cell membrane becomes "overpermeabilized" within 1 min, when irreversible damage from the surfactant occurs. Eventually the cell loses its integrity and collapses, which can be observed by SECM as a higher current in an x-scan or an approach curve very much the same as the approach taken over the dish. Solubilization of the lipid bilayer may be caused by disruption of the lipid–lipid interaction due to enhanced lipid-detergent micelle interactions. The insertion of individual detergent molecules or small aggregates at concentrations just below the CMC causes the membrane to become more permeable to a wide variety of molecules which otherwise cannot enter inside the cell allowing transfection. However at detergent concentrations where micelles form (at or above the CMC range), rapid breakdown of the membrane occur (11, 28–31).

Materials and Methods

Chemicals. All of the chemicals were used as received. $K_4[Fe(CN)_6] \cdot 3H_2O$, $MgSO_4$, $CaSO_4$ and K_2SO_4 were obtained from Fisher Scientific. D-glucose, HEPES and TX100 (T 9284) were from Sigma-Aldrich. All solutions were made with 18 MΩ Milli-Q (Millipore) reagent water.

Cell Culture. HeLa cells were purchased from ATCC (catalog number CCL-2) and cultured as per instructions provided by ATCC. In brief, cells were grown and maintained in "ATCC-formulated Eagle's Minimum Essential Medium" (ATCC 30-2003) culture medium supplemented with 10% fetal bovine serum (ATCC 30-2020) on tissue culture Petri dish (Falcon 353801). Temperature was maintained at 37 °C in a water jacketed incubator (model 2310, VWR Scientific) with 95% air and 5% CO_2.

Cell coverage of about 50% on the Petri dish was used in all the experiments. When appropriate cell coverage was obtained, the dish was taken out of the incubator and the cells were washed with buffer solution (10mM HEPES, 5.55 mM glucose, 75 mM Na_2SO_4, 1 mM $MgSO_4$ and 3 mM K_2SO_4) twice and then incubated with 1 mL of buffer solution at room temperature for 1 h. The buffer solution was then replaced by the appropriate experimental solution prepared with buffer.

Fluorescent Based Viability Assay. The fluorescent based viability assay kit (Biotium Inc.) was used to detect living and dead cells simultaneously in the sample. This assay employs two dyes, calcein AM (green dye) and EthD-III (red dye). Calcein AM has the ability to pass through an intact cell membrane and react with the intracellular enzyme esterase, which converts it into an intensely green fluorescent calcein dye (excitation/emission 495 nm/515 nm). The polyanionic calcein dye remained confined inside intact cell membranes so the living cells were easily visible though an inverted microscope (Eclipse TE300 Nikon Inverted Microscope, Melville, NY). EthD-III could permeate only through damaged membranes and reacted with intracellular nucleic acid to emit intense red fluorescence inside dead cells (excitation/emission 530 nm/635 nm). This assay was very useful for detecting both live and dead cells at the same time without any pretreatment of the samples. In this work, 1 mL of 2 μM calcein AM and 4 μM EthD-III was used to detect the viability of the cells either without, or in presence of, different concentrations of TX100 for different periods of time. The green and red stained cell photos were then processed by Image J software (available from the NIH website) to count the number of live and dead cells.

SECM Experiments. ***Electrochemistry and electrode fabrication.*** Ultramicroelectrodes (UME) of 10 μm diameter platinum wire disks (Goodfellow Cambridge Limited, UK) were used in the experiments. Detailed steps for fabrication and characterization have been reported elsewhere (15). 0.5 mm Pt wire (Goodfellow Cambridge Limited, UK) and Hg/Hg_2SO_4 (Radiometer, Copenhagen) were used as counter and reference electrodes respectively. All potentials reported here were referred to Hg/Hg_2SO_4. The SECM (model 900B, CH Instruments, Austin, TX) was used for all electrochemical experiments.

X-scan over single cell experiment. HeLa cells were cultured in approximately one 1 cm spot on the petri dish inside the incubator until the cell coverage

was about 50%. The cells were washed with buffer solution twice and then incubated with buffer solution for 1–2 h at room temperature. During that time period the petri dish with cells, tip, reference electrode, and counter electrode were set up on a SECM stage as shown in Fig. 1. The buffer-only solution was then replaced by a 4 mM ferrocyanide solution prepared with the same buffer. Approach curves were obtained at 0.5 V at three different points outside the cellular spot to adjust the tilt of the SECM stage. Tip-substrate (petri dish) distance, as shown in Fig. 1, was determined by negative feedback approach curve using Fe(II)/Fe(III) as redox couple (Fig. 2 *A* and *B*). The HeLa cells were then located by constant height (16–20 μm) SECM imaging with ferrocyanide as redox mediator at 0.5 V (Fig. 2*C*). The location of a single cell in the x-y direction was then narrowed down by x and y scanning of the tip at a fixed height (~16 μm) and potential (at 0.5 V) over the cell at a speed of 5 μm/s. No TX100 was added to the cells at this time. After identifying a cell, the 4 mM redox solution was then replaced by a solution containing different concentrations of TX100 along with 4 mM ferrocyanide. An x-direction scan was then carried out over that particular single cell several times.

Approach curve over single cell experiment. The method was nearly identical to that above. In brief the cells were found by SECM imaging and then the x-y scan was zoomed in for higher resolution. The tip was then moved above a cell and an approach curve was done at 0.5 V over the single cell with 4 mM ferrocyanide only in the solution to obtain topographic information. The redox solution then was replaced by different concentrations of TX100 and 4 mM ferrocyanide solution and approach curve experiments were performed over the cell for different periods of time.

I-t experiment over single cell. The cells were first put on the SECM stage and approach curve and x-scan experiments were performed with redox mediator only in solution as described previously. The 10 μm Pt tip was then held at a constant height (~5 μm above the highest point of the cell) and current was recorded at a constant potential of 0.5 V for 120 s every 5 min. The current in the bulk solution, 500 μm away from the cells, was also recorded by following the same procedures.

Simulation. The simulation was performed with Comsol Multiphysics 3.3 on a 2.8 GHz Intel Pentium IV processor and 2 GB RAM desktop PC. Details about the simulation model are given in *SI Text*.

Conclusions

Any concentration of TX100 at or above its CMC concentration (0.18 to 0.24 mM) in the solution is fatal to HeLa cells. This can be observed by SECM and confirmed by fluorescent tests. Damage to the cell membrane was irreversible when the cells were exposed to TX100 concentrations above CMC concentration for 10 to 30 s. However, no such effect on cell membrane permeability was observed at a concentration significantly lower (<0.15 mM) than the CMC.

When the concentration of TX100 was at or near 0.17 mM, the HeLa cell membranes became permeable after an exposure of less than 20 min. After this exposure, the cells were able to recover upon removal of surfactant solution. The permeability was estimated to be $6.5 \pm 2.0 \times 10^{-6}$ m^2/s when exposed to 0.17 mM TX100 for 32 min. Within this permeability range highly charged hydrophilic redox molecules, such as ferrocyanide, were able to pass through a live cell membrane, which would otherwise be an impermeable barrier to these redox mediators. The number of ferrocyanide molecules passed through single cell membrane after 32 min was calculated to be $1.06 \pm 0.54 \times 10^6$ in presence of 0.17 mM TX100. Thus SECM can provide not only cell viability information at the single cell level but can also give quantitative information about the cell membrane permeability. The generality of these guidelines for transfection of other cells is under investigation.

ACKNOWLEDGMENTS. We thank the National Science Foundation (CHE 0808927) and the Robert A. Welch Foundation (F-0021) for support of this work.

1. Gennuso F, et al. (2004) Bilirubin protects astrocytes from its own toxicity by inducing up-regulation and translocation of multidrug resistance-associated protein 1 (mrp1). *Proc Natl Acad Sci USA* 101:2470–2475.
2. Rajagopal A, Pant AC, Simon SM, Chen Y (2002) In Vivo analysis of human multidrug resistance protein (MRP1) activity using transient expression of fluorescently Tagged MRP1. *Cancer Res* 62:391–396.
3. Hipfner DR, Gauldie SD, Deeley RG, Cole SPC (1994) Detection of the *M*, 190,000 multidrug resistance protein, MRP, with monoclonal antibodies. *Cancer Res* 54:5788–5792.
4. Borner MM, et al. (1994) The detergent TX100 induces a death pattern in human carcinoma cell lines that resembles cytotoxic lymphocyte-induced apoptosis. *FEBS Lett* 353:129–132.
5. Benoit J, Cormier M, Wepierre J (1988) Comparative effects of four surfactants on growth, contraction and adhesion of cultured human fibroblasts. *Cell Biol Toxicol* 4(1):111–122.
6. Dayeh VR, Chow SL, Schirmer K, Lynn DH, Bols NC (2004) Evaluating the toxicity of TX100 to protozoan, fish, and mammalian cells using fluorescent dyes as indicators of cell viability. *Ecotox Environ Safe* 57:375–382.
7. Laouar L, Lowe KC, Mulligan BJ (1996) Yeast response to nonionic surfactants. *Enzyme Microb Tech* 18:433–438.
8. Barnett SM, Dracheva S, Hendler RW, Levin IW (1996) Lipid-induced conformational change of an integral membrane protein: An infrared spectroscopic study of the effects of TX100 treatment on the purple membrane of Halobacterium halobium ET1001. *Biochemistry* 35:4558–4567.
9. Aránzazu MP, Ostolaza H, Goñi FM, Barberá-Guillem E (1990) Surfactant-induced cell toxicity and cell lysis a study using B16 melanoma cells. *Biochem Pharmacol* 40(6):1323–1328.
10. Benoit J, Cormier M, Wepierre J (1988) Comparative effects of four surfactants on growth, contraction and adhesion of cultured human fibroblasts. *Cell Biol Toxicol* 4(1):111–122.
11. Maire ML, Champeil P, Moller JV (2000) Interaction of membrane proteins and lipids with solubilizing detergents. *Biochim Biophys Acta* 1508:86–111.
12. Fontaine P, et al. (2007) Unexpected stability of phospholipid langmuir monolayers deposited on TX100 aqueous solutions. *Langmuir* 23:12959–12965.
13. Nyholm T, Slotte JP (2001) Comparison of TX100 penetration into phosphatidylcholine and sphingomyelin mono- and bilayers. *Langmuir* 17:4724–4730.
14. London E, Brown DA (2000) Insolubility of lipids in TX100: Physical origin and relationship to sphingolipid/cholesterol membrane domains (rafts). *Biochim Biophys Acta* 1508:182–195.
15. Bard AJ, Mirkin MV, eds. (2001) *Scanning Electrochemical Microscopy* (Mercel Dekker, New York).
16. Li X, Bard AJ (2009) Scanning electrochemical microscopy of HeLa cells—Effects of ferrocene methanol and silver ion. *J Electroanal Chem* 628:35–42.
17. Guo J, Amemiya S (2005) Permeability of the nuclear envelope at isolated Xenopus Oocyte nuclei studied by scanning electrochemical microscopy. *Anal Chem* 77(7): 2147–2156.
18. Hirano Y, et al. (2008) Construction of time-lapse scanning electrochemical microscopy with temperature control and its applications to evaluate the preservation effects of antifreeze proteins on living cells. *Anal Chem* 80:9349–9354.
19. Gonsalves M, Macpherson JV, O'Hare D, Winlove CP, Unwin PR (2000) High resolution imaging of the distribution and permeability of methyl viologen dication in bovine articular cartilage using scanning electrochemical microscopy. *BBA-Gen Subjects* 1524(1):66–74.
20. Gonsalves M, et al. (2000) Scanning electrochemical microscopy as a local probe of oxygen permeability in cartilage. *Biophys J* 78:1578–1588.
21. London E, Brown DA (2000) Insolubility of lipids in TX100: Physical origin and relationship to sphingolipid/cholesterol membrane domains (rafts). *Biochim Biophys Acta* 1508:182–195.
22. Lanyi JK (1973) Influence of electron transport on the interaction between membrane lipids and TX100 in halobacterium cutirubrum. *Biochemistry* 12(7):1433–1438.
23. Maire ML, Champeil P, Moller JV (2000) Interaction of membrane proteins and lipids with solubilizing detergents. *Biochim Biophys Acta* 1508:86–111.
24. Fontaine P, et al. (2007) Unexpected stability of phospholipid langmuir monolayers deposited on TX100 aqueous solutions. *Langmuir* 23:12959–12965.
25. Troiano GC, Tung L, Sharma V, Stebe JK (1998) The reduction in electroporation voltages by the addition of a surfactant to planar lipid bilayers. *Biophys J* 75:880–888.
26. Sigma-Aldrich Co (1999) *TX100, T9284 product information sheet* (Sigma-Aldrich, St. Louis).
27. Rafat M, et al. (2008) Association (micellization) and partitioning of aglycon triterpenoids. *J Colloid Interface Sci* 325(2):324–330.
28. Morandat S, Kirat EK (2006) Membrane resistance to TX100 explored by real time atomic force microscopy. *Langmuir* 22:5786–5791.
29. Paternostre MT, Roux M, Rigaud JL (1988) Mechanisms of membrane protein insertion into liposomes during reconstitution procedures involving the use of detergents. 1. Solubilization of large unilamellar liposomes (prepared by reverse-phase evaporation) by TX100, Octyl Glucoside, and Sodium Cholate. *Biochemistry* 27:2668–2677.
30. Rigaud JL, Paternostre MT, Bluzat A (1988) Mechanisms of membrane protein insertion into liposomes during reconstitution procedures involving the use of detergents. 2. Incorporation of the light-driven proton pump bacteriorhodopsin. *Biochemistry* 27:2677–2688.
31. Nyholm T, Slotte JP (2001) Comparison of TX100 penetration into phosphatidylcholine and sphingomyelin mono- and bilayers. *Langmuir* 17:4724–4730.